ROZPRAWY INŻYNIERSKIE • ENGINEERING TRANSACTIONS • 37, 1, 117-136, 1989
Polska Akademia Nauk • Instytut Podstawowych Problemów Techniki

MODE INTERACTION IN WIDE PLATE WITH ANGLE SECTION LONGITUDINAL STIFFENERS UNDER COMPRESSION

Z. KOŁAKOWSKI (ŁÓDŹ)

Interaction of nearly simultaneous buckling modes in the presence of imperfections is studied. The investigation is concerned with infinitely wide plate with thin-walled angle longitudinal stiffeners under uniform compression.

The asymptotic expansion established by BYSKOV and HUTCHINSON [1] is also used here. The present paper is devoted to the improved study of equilibrium path in the initial postbuckling behaviour of imperfect structures with regard to the effect of interaction of the global mode and two local buckling modes.

NOTATION

l length of the stiffened plate,
b_i width of wall i of the plate,
h_i thickness of wall i of the plate,
E Young's modulus,
D_i flexural rigidity of wall i,
u_i, v_i, w_i displacements of middle surface,
$\mathring{u}_i, \mathring{v}_i, \mathring{w}_i$ prebuckling displacement fields,
$\overset{n}{u}_i, \overset{n}{v}_i, \overset{n}{w}_i$ buckling displacement fields,
Δ measure of the applied pressure,
N_{ix}, N_{iy}, N_{ixy} in-plane stress resultants for wall i,
M_{ix}, M_{iy}, M_{ixy} bending moment resultants for wall i,
Q_{iy} Eq. (2.5),
n number of mode,
m number of axial half-waves of mode number n,
λ scalar load parameter,
λ_n value of λ at bifurcation mode number n,
λ_s maximum value of λ for imperfect stiffened plate,
ξ_n amplitude of buckling mode number n,
$\bar{\xi}_n$ imperfection amplitude corresponding to ξ_n,
$\sigma_n^* = \dfrac{\sigma_n 10^3}{E}$ dimensionless stress of mode number n,
σ_s^* dimensionless limit stress,
σ_m^* min (σ_1^*, σ_2^*),
a_{ijJ} postbuckling coefficients (see BYSKOV and HUTCHINSON [1]),
d_2 a_{221},
d_3 $a_{122}+a_{212}$.

1. Introduction

Interaction between the buckling modes may result in an imperfection-sensitively structure and is the principal cause of collapse of thin-walled structures.

In recent years more and more papers have been devoted to the analysis of the interaction of buckling modes as a factor that determines the construction imperfection sensitivity at nearly the same magnitudes of bifurcational loads corresponding to different buckling modes and to the closely related problem of optimum structural design.

The constructions shaped as an infinitely wide plate strengthened by longitudinal stiffeners have been analysed in the most detailed manner with the application of general methods of stability analysis of constructions, susceptible to imperfections [1–8].

The general theory of interaction of buckling modes of stiffened plates was developed by Koiter [2] by means of a generalization of the approach [3]. Koiter and Van der Neut [9] proposed a technique in which the interaction of an overall mode with two local modes having the same wavelength were considered. The fundamental mode is henceforth called "primary" and the nontrivial higher mode (having the same wavelength as the "primary") corresponding to the mode triggered by the overall long-wave mode is called "secondary".

The previous paper [10] was devoted to an analysis of the initial post buckling behaviour of a wide plate with the thin-walled trapezoidal section stiffeners. In the following paper [11] the difference between the two- and three-mode approach has been shown.

As the effect of shear lag is more pronounced in stiffened plates than in unstiffened plates of the same extensional rigidity, the designer is even more concerned with the interaction of shear lag and collapse by buckling in the case of wide stiffened flanges.

The possibility of dangerous interaction of the global and the local buckling modes for finite displacements gives rise to another question: how to reduce those interactions and how to estimate their efficiency. One way of accomplishing these goals consists in using angle profile stiffeners.

In the present paper the initial post-buckling behaviour of wide plates with thin-walled angle section stiffeners being under compression in the elastic range is examined on the basis of Byskov and Hutchinson's method with the cooperation between all the walls of the structures being taken into account. The obtained solutions include the effect of interaction of two modes having the same wavelength, shear lag and cross-sectional distortions.

2. Structural problem

A simply supported plate of infinite width with the angle section of longitudinal regularly arranged stiffeners is considered in the present paper.

The type of cross-section of this structure consists of a few flat plates with a perpendicular axis of symmetry and the assumed local coordinate systems are presented in Fig. 1.

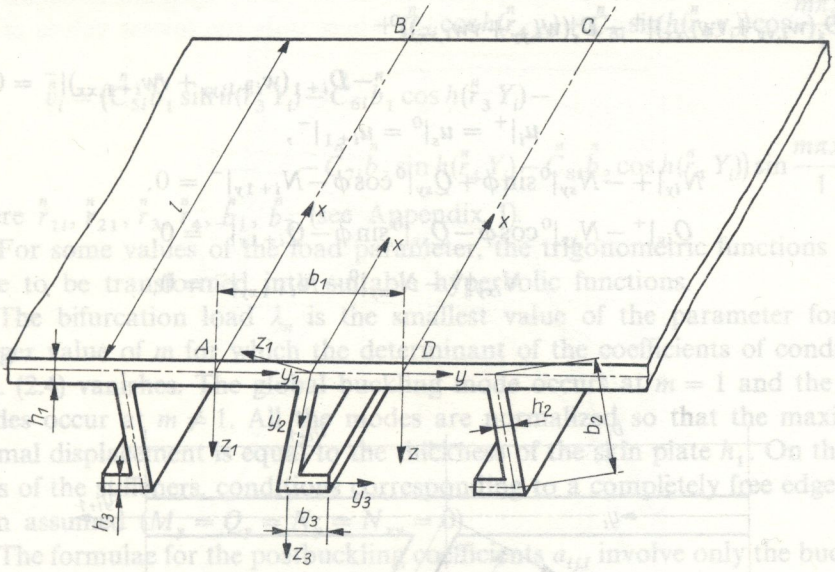

FIG. 1. Part of wide plate with longitudinal stiffeners.

The material of the stiffened plate obey Hooke's law.

The membrane strains of the wall i are obtained as

$$\varepsilon_{ix} = u_{i,x} + 0.5(w_{i,x}^2 + v_{i,x}^2),$$
$$\varepsilon_{iy} = v_{i,y} + 0.5(w_{i,y}^2 + u_{i,y}^2), \tag{2.1}$$
$$\gamma_{ixy} = u_{i,y} + v_{i,x} + w_{i,x} w_{i,y}$$

and the bending strains are given by

$$\varkappa_{ix} = -w_{i,xx}, \quad \varkappa_{iy} = -w_{i,yy}, \quad \varkappa_{ixy} = -w_{i,xy}. \tag{2.2}$$

The differential equilibrium equations resulting from the virtual work expression for one wall can be written as

$$-N_{ix,x} - N_{ixy,y} - (N_{iy} u_{i,y})_{,y} = 0,$$
$$-N_{iy,y} - N_{ixy,x} - (N_{ix} v_{i,x})_{,x} = 0, \tag{2.3}$$
$$D_i \nabla\nabla w_i - (N_{ix} w_{i,x})_{,x} - (N_{iy} w_{i,y})_{,y} - (N_{ixy} w_{i,x})_{,y} - (N_{ixy} w_{i,y})_{,x} = 0.$$

The geometrical and statical continuity conditions at the junctions of plates (Fig. 2) may be written as

$$
\begin{aligned}
&w_i|^+ = w_s|^0 \sin\phi + v_s|^0 \cos\phi = w_{i+1}|^-,\\
&v_i|^+ = v_s|^0 \sin\phi - w_s|^0 \cos\phi = v_{i+1}|^-,\\
&w_{i,y}|^+ = w_{s,y}|^0 = w_{i+1,y}|^-,\\
&D_i(w_{i,yy} + \nu w_{i,xx})|^+ - D_s(w_{s,yy} + \nu w_{i,xx})|^0\\
&\qquad - D_{i+1}(w_{i+1,yy} + \nu w_{i+1,xx})|^- = 0,\\
&u_i|^+ = u_s|^0 = u_{i+1}|^-,\\
&N_{iy}|+ - N_{sy}|^0 \sin\phi + Q_{sy}|^0 \cos\phi - N_{i+1y}|^- = 0,\\
&Q_{iy}|^+ - N_{sy}|^0 \cos\phi - Q_{sy}|^0 \sin\phi - Q_{i+1y}|^- = 0,\\
&N_{ixy}|^+ - N_{sxy}|^0 - N_{i+1xy}|^- = 0,
\end{aligned}
\tag{2.4}
$$

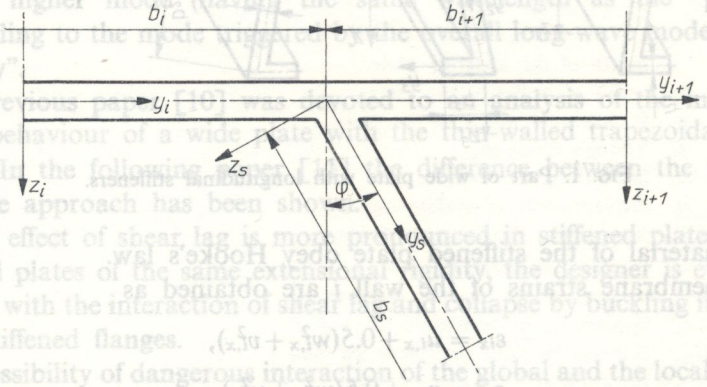

FIG. 2. Local coordinate systems for each plate meeting at the corner.

where

$$Q_{iy} = N_{iy} w_{i,y} + N_{ixy} w_{i,x} - D_i(w_{i,yyy} + (2-\nu) w_{i,xxy}). \tag{2.5}$$

The prebuckling solution consists of homogeneous fields and we may take

$$\mathring{u}_i = -x_i \Delta, \quad \mathring{v}_i = \nu y_i \Delta, \quad \mathring{w}_i = 0. \tag{2.6}$$

The boundary conditions permit the first order solution to be written as

$$
\begin{aligned}
\overset{n}{w}_i &= (\overset{n}{C}_{1i}\cosh(\overset{n}{r}_{1i}y_i)+\overset{n}{C}_{2i}\sinh(\overset{n}{r}_{1i}Y_i)+\overset{n}{C}_{3i}\cos(\overset{n}{r}_{2i}Y_i)+ \\
&\qquad +\overset{n}{C}_{4i}\sin(\overset{n}{r}_{2i}y_i))\sin\frac{m\pi x_i}{1}, \\
\overset{n}{u}_i &= (\overset{n}{C}_{5i}\cosh(\overset{n}{r}_3 y_i)+\overset{n}{C}_{6i}\sinh(\overset{n}{r}_3 y_i)+ \\
&\qquad +\overset{n}{C}_{7i}\cosh(\overset{n}{r}_4 y_i)+\overset{n}{C}_{8i}\sinh(\overset{n}{r}_4 y_i))\cos\frac{m\pi x_i}{1}, \\
\overset{n}{v}_i &= (\overset{n}{C}_{5i}\overset{n}{b}_1\sinh(\overset{n}{r}_3 Y_i)-\overset{n}{C}_{6i}\overset{n}{b}_1\cosh(\overset{n}{r}_3 Y_i)- \\
&\qquad -\overset{n}{C}_{7i}\overset{n}{b}_2\sinh(\overset{n}{r}_4 Y_i)-\overset{n}{C}_{8i}\overset{n}{b}_2\cosh(\overset{n}{r}_4 Y_i))\sin\frac{m\pi x_i}{1},
\end{aligned}
\tag{2.7}
$$

where $\overset{n}{r}_{1i}, \overset{n}{r}_{21}, \overset{n}{r}_3, \overset{n}{r}_4, \overset{n}{b}_1, \overset{n}{b}_2$ (see Appendix I).

For some values of the load parameter, the trigonometric functions $(2.7)_1$ have to be transformed into suitable hyperbolic functions.

The bifurcation load λ_n is the smallest value of the parameter for any integer value of m for which the determinant of the coefficients of conditions Eqs. (2.4) vanishes. The global buckling mode occurs at $m = 1$ and the local modes occur at $m \neq 1$. All the modes are normalized so that the maximum normal displacement is equal to the thickness of the skin plate h_1. On the free ends of the stiffeners, conditions corresponding to a completely free edge have been assumed ($M_y = Q_y = N_y = N_{xy} = 0$).

The formulae for the postbuckling coefficients a_{ijJ} involve only the buckling modes. In the points where the scalar load parameter λ_s reaches the maximum value for imperfect structure (bifurcation or limit points), the Jacobian of system of nonlinear equations [1] (see Appendix II):

$$
\xi_J(1-\lambda/\lambda_J)+\xi_i\xi_j a_{ijJ}+\ldots = \lambda/\lambda_J\xi_J \quad \text{at} \quad J = 1, \ldots, n \tag{2.8}
$$

is equal to zero.

The symbols, formulae and methods of the solution applied in this paper are identical to those in the paper [10].

3. Results

Detailed numerical calculations for some wide plates with thin-walled longitudinal stiffeners, the geometry of which is known from literature [8, 11, 12], have been performed.

Because of the symmetry with respect to the longitudinal centre lines of each skin plate, only the action of a typical panel included between two successive centre lines is considered.

Let us take into account a wide plate strengthened with regularly displaced angle ribs, the dimensions of their cross section [12] (Fig. 1) being

$$b_1/b_2 = 0.5, \quad h_1/h_2 = 1.0, \quad h_1/h_3 = 1.0, \quad l/b_1 = 13.2,$$
$$b_1/h_1 = 50.0 \quad \phi = 0^0.$$

Figure 3 presents the dimensionless stress $\sigma_n^*(\nu = 0.3)$ as a function of the width of the angle stiffener flange b_3/b_2. A circle in the latter diagram indicates the results which have been obtained in [12] where only the lowest values of the

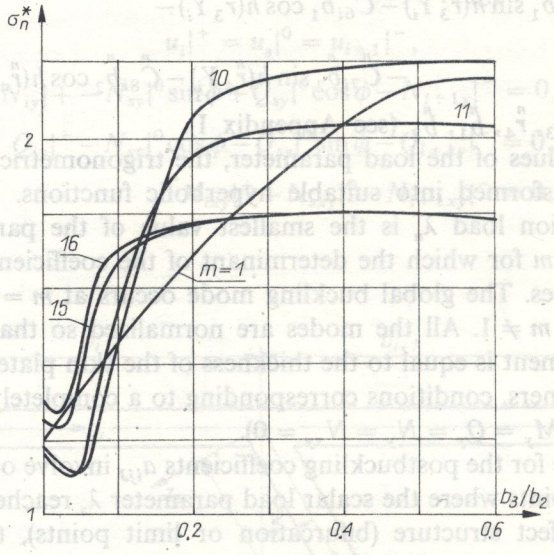

FIG. 3. Dimensionless stresses σ_n^* carried by the width of the angle stiffener flange b_3/b_2 for different buckling modes.

load σ^* are reported for a given value of b_3/b_2. The plot can be divided into four parts. The significance of Interval I, $0 \leqslant b_3/b_2 \leqslant 0.05$ is merely theoretical since $b_3/h_2 \leqslant 1$ for these values. The global load σ_1^* (at $m = 1$) increases in this interval as a result of an increase in the height of rectangular stiffeners ($b_2 \cong b_2 + h_3$; $b_3 \cong 0$). That, in turn, causes a reduction of local load values $\sigma_n^*(n \neq 1)$. In Interval II, $0.05 \leqslant b_3/b_2 \leqslant 0.25$, values of load σ_n^* increase rapidly. It is a consequence of the increased flexural rigidity of stiffener flanges. In Interval III, $0.25 \leqslant b_3/b_2 \leqslant 0.5$, values of local load stabilize. The flange has an influence only on torsional not on flexural rigidity. Moreover, in the same interval a further increase in global load σ_1^* takes place. Interval IV, $b_3/b_2 > 0.5$, is characterized by a slow, monotone decrease in the values of the load σ_n^*. The rib flange appears to be the "weakest" part of the stiffened plate, responsible for the loss of stability. Also the shear lag effect gains in importance and is discussed below.

Figure 4 shows the dependence of dimensionless stress σ_n^* upon the flange width b_3/b_2, other dimensions of stiffened plate being constant:

$$b_1/b_2 = 4.226, \quad h_1/h_2 = 2.367, \quad h_1/h_3 = 2.367,$$
$$l/b_1 = 2.591, \quad b_1/h_1 = 35.714, \quad \phi = 0^0.$$

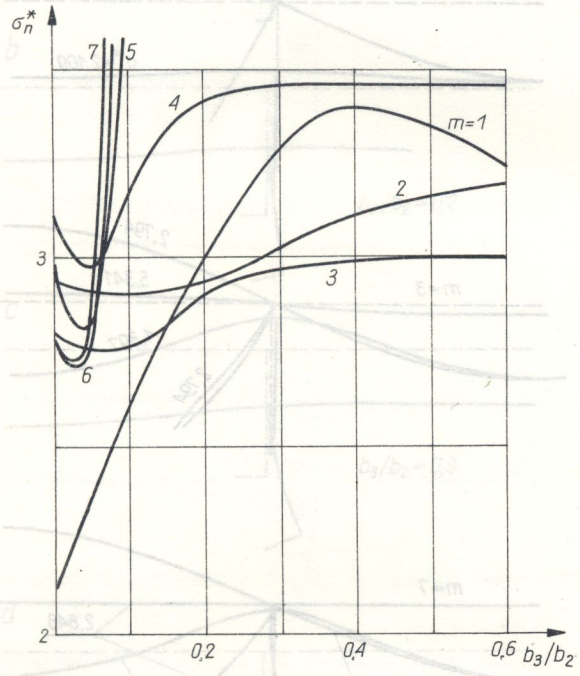

FIG. 4. Relationship between dimensionless stresses σ_n^* and the flange width b_3/b_2.

For geometrical dimensions of rectangular stiffeners ($b_3 = 0$), we have taken the same values as in the papers [7, 11]. It can easily be noticed that for the geometrical dimension $b_3/b_2 = 0$ of the stiffened plate two local buckling modes at different numbers of half waves occur almost simultaneously. In this case the primary local mode at $m = 3$ may be called "local mode of skin plate" and in the case $m = 7$ the primary local mode "local mode of stiffeners". In Fig. 4 only the Interval I ($0 \leqslant b_3/b_2 \leqslant 0.05$) can be clearly distinguished; it is identical to that in Fig. 3. In the Interval II ($0.05 \leqslant b_3/b_2 \leqslant 0.4$), however, even a weak flange makes the load values σ_n^* rise significantly. In the Interval III, where $b_3/b_2 > 0.4$, the global load σ_1^* drops sharply and there is a marked tendency to a slow decrease in local values at $m = 3, 4$. For $m = 2$ only a slow futher rise in σ^* load can be observed.

In Fig. 5a the first two overall buckling modes are shown at $b_3/b_2 = 0$ and the first three local modes at half waves $m = 3$ and $m = 7$ are presented in Figs. 5b and 5c, respectively.

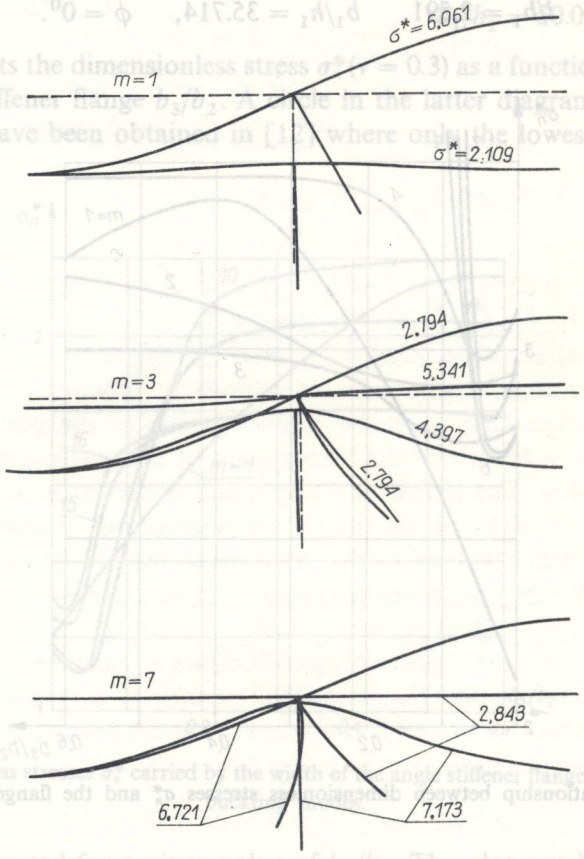

FIG. 5. Two global and several local modes for the wide plate with rectangular stiffeners.

The next diagram (Fig. 6) depicts global buckling modes ($m = 1$) of the discussed plate at different widths of strengthening flanges ($b_3/b_2 = 0.1$; 0.2; 0.3; 0.4; 0.5). One can easily find out that the wider the flange, the higher the values of stiffener deflections and the asymmetry of skin plate in relation to the stiffener web (cf. Figs. 5 and 6d). Hence the technical theory of stiffened plates [13, 14] even if used for the determination of global load values for angle stiffener-strenthened plates may lead to considerable discrepancies in comparison with the assumed, here, description of global buckling by means of nonlinear Kármán's equations.

Subsequent Figs. 7–9 present exemplary plots of in-plane stress resultants

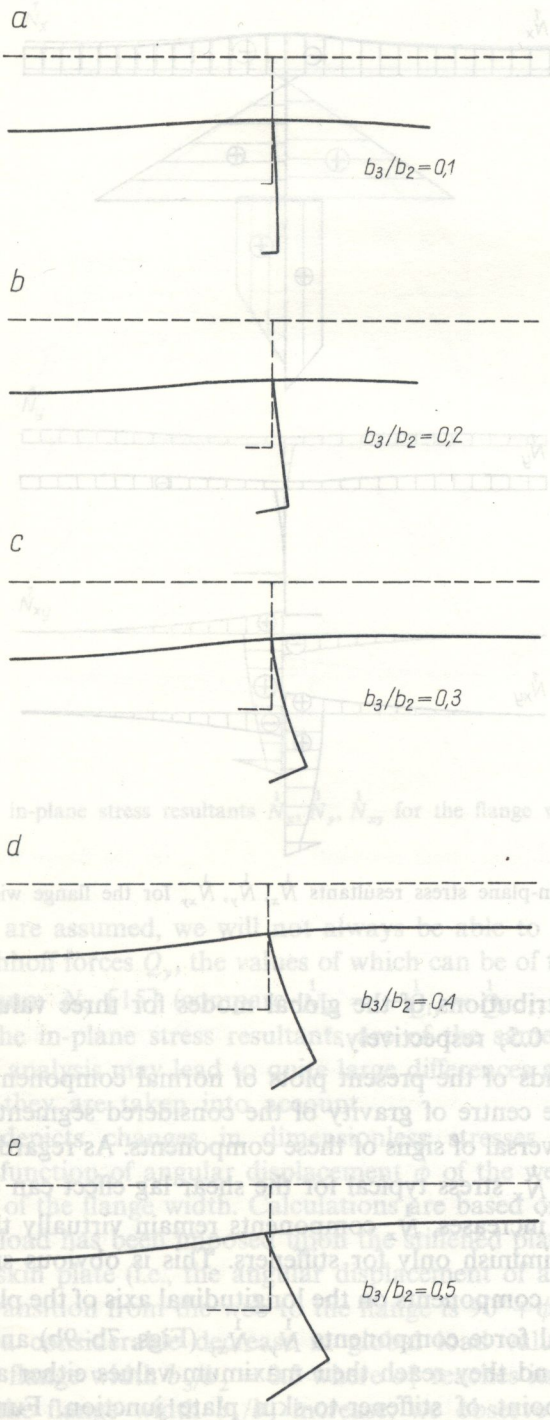

FIG. 6. Global buckling modes of stiffened plate for several flange widths b_3/b_2.

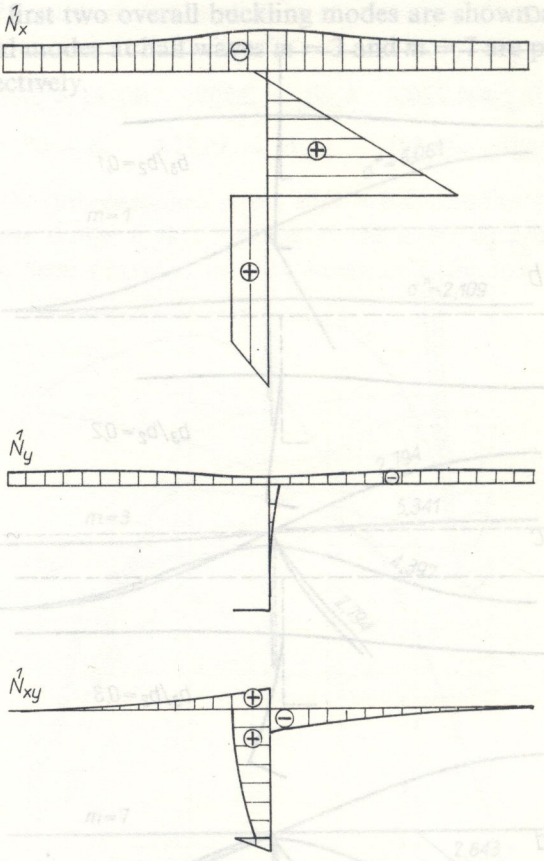

FIG. 7. Plot of in-plane stress resultants $\overset{1}{N}_x$, $\overset{1}{N}_y$, $\overset{1}{N}_{xy}$ for the flange width $b_3/b_2 = 0.3$.

$\overset{1}{N}_x$, $\overset{1}{N}_y$, $\overset{1}{N}_{xy}$, distributions of the global modes for three values of the ratios $b_3/b_2 = 0.3$; 0.4; 0.5; respectively.

On the grounds of the present plots of normal components $\overset{1}{N}_x$, it can be stated that in the centre of gravity of the considered segment *ABCD* (Fig. 1) there occurs a reversal of signs of these components. As regards the skin plate, a distribution of $\overset{1}{N}_x$ stress typical for the shear lag effect can be observed. As the flange width increases, $\overset{1}{N}_x$ components remain virtually the same for the skin plate and diminish only for stiffeners. This is obvious since the sum of projections of $\overset{1}{N}_x$ components on the longitudinal axis of the plate must always be zero. Sectional force components $\overset{1}{N}_y$, $\overset{1}{N}_{xy}$ (Figs. 7b–9b) and (7c–9c) are of the same order and they reach their maximum values either at the symmetry axis or at the point of stiffener-to-skin plate junction. Furthemore, if the simplified conditions of the cooperation between all the walls of the structures

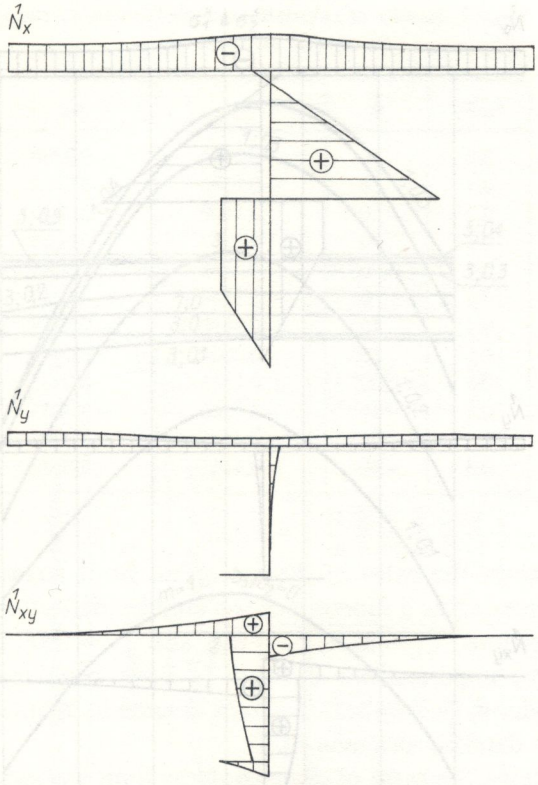

FIG. 8. Plot of in-plane stress resultants $\overset{1}{N}_x$, $\overset{1}{N}_y$, $\overset{1}{N}_{xy}$ for the flange width $b_3/b_2 = 0.4$.

at the junction are assumed, we will not always be able to neglect summary transverse Kirchhoff forces Q_y, the values of which can be of the same order as those of maximum N_y [15] (compare $\overset{1}{N}_{sy} = -\overset{1}{Q}_{iy} = \overset{1}{Q}_{i+1y}$ in Figs. 7b–9b). Summing up, the in-plane stress resultants are of the same order and their omission in the analysis may lead to quite large differences as compared with the case when they are taken into account.

Figure 10 depicts changes in dimensionless stresses σ_1^* $(m = 1)$ and $\sigma_2^*(m = 3)$ as a function of angular displacement ϕ of the web (see Fig. 2) for different values of the flange width. Calculations are based on the assumption that before the load has been imposed upon the stiffened plate, rib flanges are parallel to the skin plate (i.e., the angular displacement of a local coordinate system at the transition from the web to the flange is $90° + \phi$). Changes in the ϕ angle cause a considerable decrease in global load values σ_1^*. The only exception is the flange width $b_3/b_2 = 0.5$ where σ_1^* reaches its maximum value at $\phi \cong 7°$. As the flange width b_3/b_2 increase, we observe more and more distinct asymmetry of load σ_1^* for positive and negative values of angular

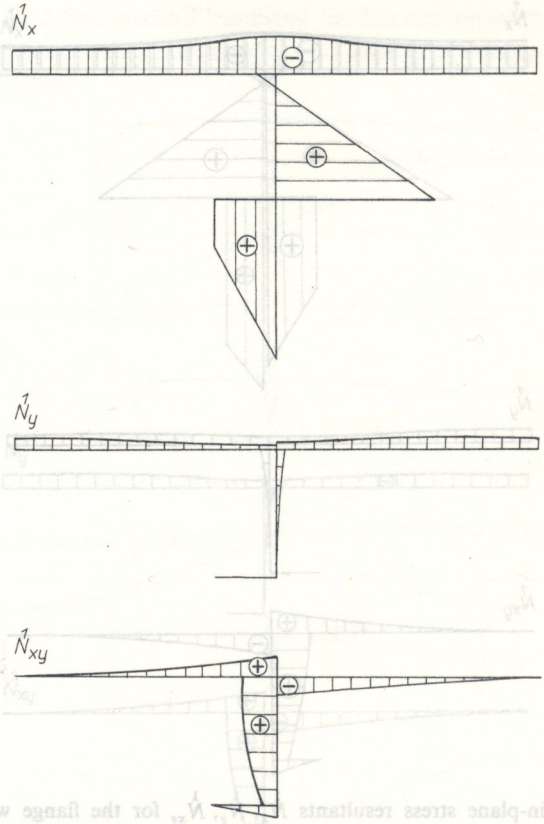

FIG. 9. Plot of in-plane stress resultants $\overset{1}{N}_x$, $\overset{1}{N}_y$, $\overset{1}{N}_{xy}$ for the flange width $b_3/b_2 = 0.5$.

displacement ϕ. This is the result of different buckling modes for different ϕ angles while the value of b_3/b_2 is fixed. At the same time the values of the local load $\sigma_2^*(m = 3)$ remain virtually constant, their changes being practically negligible. This fact can be explained in the following way. While determining approximate values of load, corresponding to the first local modes under conditions of mating, we are able to take into account only a situation where the angle is constant and the bending moments are equal; moreover, the deflection function w_i for individual plates is assumed to be zero at the points of junction.

Changes of some nonlinear coefficients (2.8) $d_2(= a_{221})$ and $d_3(= a_{122} + a_{212})$ (see [7, 8, 10, 11] for more detailed discussion) for different values of flange width b_3/b_2 and angular displacement ϕ of stiffener web are presented in Table 1. The influence of the flange width and web angular displacement on the coefficients a_{ijJ} is very complex. The coefficients are sums of integrals of

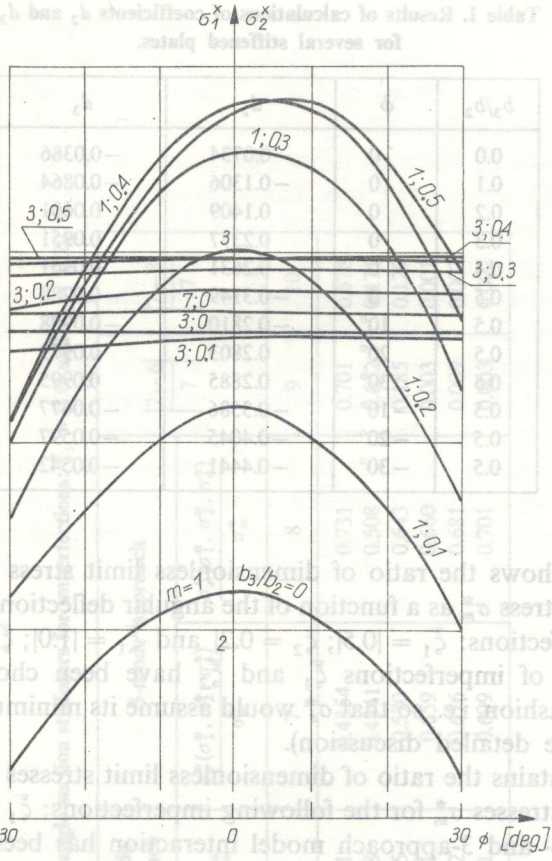

FIG. 10. Relationship between stresses σ_1^x, σ_2^x and the angular displacement ϕ of the web for several flange widths.

different signs; they depend on the ratios of displacement amplitudes of skin plate and stiffeners. As the flange width b_3/b_2 goes up, there is either a monotone increase in coefficients d_2 and d_3 or a reversal of signs. In the latter case, if b_3/b_2 is "properly" chosen, the sensitivity to imperfections can be diminished. The Byskov and Hutchinson theory applied here reduces all kinds of imperfections to such imperfections that correspond to initial deflections of a thin-walled structure; the nonlinear coefficients a_{ijj} (2.8) remain constant. However, the results for $b_3/b_2 = 0.5$ (Table 1) indicate that even a slight alteration of angular deflection ϕ of the web may bring about even a reversal of signs of those coefficients. Not all kinds of imperfections can be reduced to a single type. Calculations of slight deviations of load and geometrical dimensions allow to obtain "proper" imperfection sensitivity of constructions as well as to find out whether the assumed model of single type imperfection is correct.

Table 1. Results of calculations of coefficients d_2 and d_3 for several stiffened plates.

b_3/b_2	ϕ	d_2	d_3
0.0	0	−0.0734	−0.0386
0.1	0	−0.1306	−0.0864
0.2	0	0.1409	0.0601
0.3	0	0.2377	0.0951
0.4	0	0.2631	0.0961
0.5	0	−0.3149	−0.0788
0.5	10°	−0.2810	−0.0928
0.5	20°	0.2803	0.0979
0.5	30°	0.2885	0.0995
0.5	−10°	−0.3586	−0.0677
0.5	−20°	−0.4045	−0.0597
0.5	−30°	−0.4441	−0.0542

Figure 11 shows the ratio of dimensionless limit stress σ_s^* to the lowest dimensionless stress σ_m^* as a function of the angular deflection ϕ of web for two pairs of imperfections: $\bar{\xi}_1 = |0.5|$; $\xi_2 = 0.2|$ and $\bar{\xi}_1 = |1.0|$; $\bar{\xi}_2 = |0.2|$. In each case the signs of imperfections $\bar{\xi}_1$ and $\bar{\xi}_2$ have been chosen in the most unfavourable fashion, i.e., so that σ_s^* would assume its minimum value (see [10, 11] for a more detailed discussion).

Table 2 contains the ratio of dimensionless limit stresses σ_s^* to that lowest dimensionless stresses σ_m^* for the following imperfections: $\bar{\xi}_1 = |^{1.0}|$, $\bar{\xi}_2 = |0.2|$, $\bar{\xi}_3 = 0.0$; the 2- and 3-approach model interaction has been assumed in the calculations. The same table contains the values of dimensionless global stress $\sigma_1^*(m = 1)$ and the first three values of local stresses σ_2^*, σ_3^* σ_4^* (at $m = 3$).

On the basis of the results obtained for the wide stiffened plate, it is possible to conclude that in that case the interaction of the overall buckling mode with

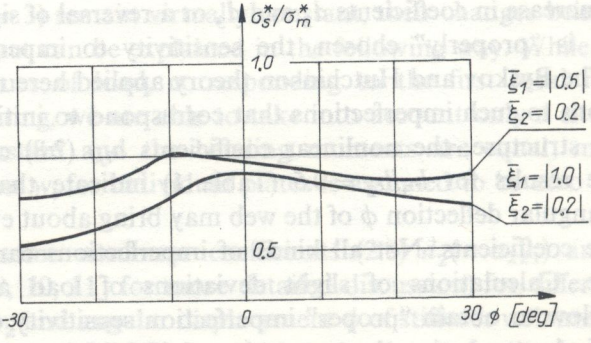

FIG. 11. Relationship between σ_s^*/σ_m^* and the angular displacement ϕ of the web for several values of $\bar{\xi}$ and $\bar{\xi}_2$.

Table 2. Dimensionless limit stresses carried by the plate with angle section stiffeners for imperfections: $\bar{\xi}_1 = |1.0|$ and $\bar{\xi}_2 = |0.2|$.

b_3/b_2	σ_1^* $(m=1)$	σ_2^* $(m=3)$	σ_3^* $(m=3)$	σ_4^* $(m=3)$	2-mode approach	3-mode approach		$\left\|\frac{7-6}{7}\right\|$	$\left\|\frac{7-8}{7}\right\|$
					σ_s^*/σ_m^*	$\frac{\sigma_s^*(\sigma_1^*, \sigma_2^*, \sigma_3^*)}{\sigma_m^*}$	$\frac{\sigma_s^*(\sigma_1^*, \sigma_2^*, \sigma_4^*)}{\sigma_m^*}$		
1	2	3	4	5	6	7	8	9	10
0.0	2.109	2.794	5.341	4.397	0.741	0.4354	0.731	0.701	0.678
0.1	2.595	2.779	4.813	4.360	0.708	0.4341	0.508	0.632	0.171
0.2	3.006	2.904	6.372	4.361	0.675	0.570	0.643	0.185	0.129
0.3	3.289	2.962	9.624	4.439	0.661	0.659	0.660	0.003	0.001
0.4	3.405	2.982	13.585	4.475	0.682	0.676	0.681	0.009	0.007
0.5	3.378	2.989	15.873	4.506	0.701	0.699	0.701	0.003	0.002

the primary and the corresponding secondary local modes triggered by overall mode (having the same shape as the global) is of great importance (for example compare cases 1 and 2 for σ_3^* and σ_4^*). This effect is contained in the term $\sigma_1 \cdot l_{11}(u_1, u_k)$ (where $l, k = 2,3$) in the coefficients a_{ijj} of Eqs. (2.8). As the imperfection $\bar{\xi}_1$ and $\bar{\xi}_2$ becomes more significant, the difference between these two approaches increases [11], too. The local mode imperfections promote an interaction between the local mode (s) and the global mode. As the second nontrivial buckling mode σ_3^* increases largely (Table 2), the differences between the 2- and 3-approach interaction model become less and less significant. This statement is valid also in the case of the 3-approach model if two different second local buckling modes are taken into account (namely σ_3^* and σ_4^*). The detailed analysis [11, 15] has proved that one needs only to consider the interaction of global buckling mode with the primary local and nontrivial secondary local modes. In order to find the most unfavourable second local buckling mode, several first values of local stresses, corresponding to a given number of half waves m, must be determined. Then the coefficients a_{ijj} for each of these values are calculated. The only way of finding the most unfavourable second local mode is by obtaining those coefficients.

4. Conclusions

The initial postbuckling behaviour of the thin-walled infinitely wide plate with the angle section stiffeners has been presented. The present approach regards the secondary local mode activated by the interaction of the overall mode with the primary local mode. Rational dimensions of angle stiffeners can be determined on the basis of the assumption of the plate model of ribs. The influence of the flange upon the nonlinear characteristic and imperfection sensitivity is related to a number of different factors. The imperfection sensitivity can be lowered provided that the flange parameters are selected entirely by means of nonlinear analysis. The assumption of a single type of imperfection is quite questionable. In the case when a few buckling modes are comparable, disregarding of mode interaction may lead to overstimating the load carrying capacity of the structure.

Appendix I

$$\overset{n}{r}_{1i} = \left[-\frac{m\pi}{l}\left[\frac{m\pi}{l} + \sqrt{\frac{12(1-\nu^2)\lambda\Delta}{h_i^2}}\right]\right]^{1/2},$$

$$\overset{n}{r}_{2i} = \left[\frac{-m\pi}{l}\left[\frac{m\pi}{l} - \sqrt{\frac{12(1-\nu^2)\lambda\Delta}{h_i^2}}\right]\right]^{1/2},$$

$$\overset{n}{e}_1 = \frac{1-\nu}{2},$$

$$\overset{n}{e}_2 = (1-\nu)\left(\frac{m\pi}{l}\right)^2\left(\frac{1-\nu^2}{2}\lambda\Delta - 1\right),$$

$$\overset{n}{e}_3 = (1-\nu^2)^2\left(\frac{m\pi}{l}\right)^4\left[\frac{1}{4}\lambda^2\Delta^2(1-\nu^2)+\lambda\Delta\right],$$

$$\overset{n}{r}_3 = \left[\frac{-\overset{n}{e}_2+\sqrt{\overset{n}{e}_3}}{2\overset{n}{e}_1}\right]^{1/2},$$

$$\overset{n}{r}_4 = \left[\frac{-\overset{n}{e}_2-\sqrt{\overset{n}{e}_3}}{2\overset{n}{e}_1}\right]^{1/2},$$

$$\overset{n}{b}_1 = \frac{1-\nu}{1+\nu}\cdot\frac{\overset{n}{r}_3}{\dfrac{m\pi}{l}} - \frac{2\dfrac{m\pi}{l}}{\overset{n}{r}_3(1+\nu)},$$

$$\overset{n}{b}_2 = \frac{1-\nu}{1+\nu}\cdot\frac{\overset{n}{r}_4}{\dfrac{m\pi}{l}} - \frac{2\dfrac{m\pi}{l}}{\overset{n}{r}_4(1+\nu)},$$

Appendix II

The method outlined in the following was developed by Byskov and Hutchinson in [1] where a complete derivation is given. This method is suitable for structures with M simultaneous or nearly simultaneous buckling modes.

Assume that the structure is perfect and that the prebuckling state is linear with respect to the scalar load parameter λ. The displacement field is expanded in the following fashion:

$$u = \lambda u_0 + \xi_i u_i + \xi_i\xi_j u_{ij} + \ldots, \tag{A.1}$$

where the prebuckling displacement field is described by λu_0, the amplitude ξ_i measures the influence of the buckling mode u_i, and u_{ij} is the second order field associated with u_i and u_j. Summation from 1 to M is implied for repeated Latin lower-case indices.

The stress and strain fields are expanded in a fashion similar to (A.1):

$$\begin{aligned}\sigma &= \lambda\sigma_0 + \xi_i\sigma_i + \xi_i\xi_j\sigma_{ij} + \ldots,\\ \varepsilon &= \lambda\varepsilon_0 + \xi_i\varepsilon_i + \xi_i\xi_j\varepsilon_{ij} + \ldots.\end{aligned} \tag{A.2}$$

The strain-displacement relation can be written in the form

$$\varepsilon = l_1(\mu) + 0.5 l_2(u), \tag{A.3}$$

where l_1 and l_2 are linear and quadratic operators, respectively. A bilinear operator l_{11} is defined by

$$l_2(u+v) = l_2(u) + 2l_{11}(u, v) + l_2(v). \tag{A.4}$$

The linearity of the prebuckling state is characterized by

$$l_{11}(u_0, v) = 0 \tag{A.5}$$

for any v which in turn implies

$$\varepsilon_0 = l_1(u_0). \tag{A.6}$$

The material is assumed to be linearly elastic so that the stress σ is given by

$$\sigma = H(\varepsilon) \tag{A.7}$$

where H designates a linear operator.

The dot notation used in the following denotes integration over the entire structure:

$$\sigma \cdot \varepsilon = \int_v \sigma_{ij}\varepsilon_{ij} dv. \tag{A.8}$$

The eigenvalue problems determining the buckling modes and their associated eigenvalues λ_J are found from the variational equation

$$\sigma_J \cdot l_1(\delta u) + \lambda_J \sigma_0 \cdot l_{11}(u_J, \delta u) = 0, \quad J = 1, \ldots, M, \tag{A.9}$$

where δu denotes all kinematically admissible variations of u. The buckling modes are taken to be mutually orthogonal in the following sense:

$$\sigma_0 \cdot l_{11}(u_i, u_j) = 0, \quad i \neq j. \tag{A.10}$$

The second order and all possible order fields may be shown to be orthogonal to all buckling modes in the sense of (A.10). For a displacement field u the amplitude ξ_J of its component in the shape of u_J is defined by

$$\sigma_0 \cdot l_{11}(u, u_J) = \xi_J \sigma_0 \cdot l_2(u_J). \tag{A.11}$$

A variational statement of the second-order boundary value problems is

$$\sigma_{ij} \cdot l_1(\delta u) + \lambda \sigma_0 \cdot l_{11}(u_{ij}, \delta u) = -0.5(\sigma_i \cdot l_{11}(u_j, \delta u) + \sigma_j \cdot l_{11}(u_i, \delta u)), \tag{A.12}$$

where u_{ij} and δu are orthogonal to each u_k in the sense of (A.10) and $\lambda = \lambda_c = \min(\lambda_J)$.

The right hand side of this expression is symmetric in their indices.

If the structure suffers geometric imperfections $\bar{u}$ given by

$$\bar{u} = \bar{\xi}_i u_i, \tag{A.13}$$

the following M nonlinear equations determine the equilibrium path

$$\text{(A.14)} \qquad \xi_J\left(1-\frac{\lambda}{\lambda_J}\right)+\xi_i\xi_j a_{ijJ}+\xi_i\xi_j\xi_k b_{ijkJ}=\frac{\lambda}{\lambda_J}\bar{\xi}_J, \qquad J=1,..,M.$$

The formulas for the coefficients are

$$a_{ijJ}=[\sigma_J\cdot l_{11}(u_i,u_j)+2\sigma_i\cdot l_{11}(u_j,u_J)]/(2\sigma_J\cdot\varepsilon_J)$$

and

$$\text{(A.15)} \qquad b_{ijkJ}=[\sigma_{Ji}\cdot l_{11}(u_j,u_k)+\sigma_{ij}l_{11}(u_k,u_J)+\sigma_J\cdot l_{11}(u_i,u_{jk})$$
$$+\sigma_i\cdot l_{11}(u_J,u_{jk})+2\sigma_i\cdot l_{11}(u_j,u_{kJ})]/(2\sigma_J\cdot\varepsilon_J).$$

REFERENCES

1. E. BYSKOV, J. W. HUTCHINSON, *Mode interaction in axially stiffened cylindrical shells*, AIAA J., **15**, 7, 1977.
2. W. T. KOITER, *General theory of mode interaction in stiffened plate and shell structures*, WTHD, Report 590, Delft, Holland 1976.
3. W. T. KOITER, M. PIGNATARO, *An alternative approach to the interaction between local and overall buckling in stiffened panels*, Buckling of Struct., Proc. IUTAM, Symposium, 1976.
4. F. W. WILLIAMS, W. H. WITTRICK, R. J. PLANK, *Critical buckling loads of some prismatic plate assemblies*, Buckling of Struct., Proc. IUTAM, Symposium, 1976.
5. W. C. FOK, J. RHODES, A. C. WALKER, *Local buckling of outstands in stiffened plates*, Aeronaut. Quart., **127**, 1976.
6. W. C. FOK, A. C. WALKER, J. RHODES, *Buckling of locally imperfect stiffeners in plate*, J. Eng. Mech. Div., Proc. Amer. Soc. Civ. Eng., **103**, 5, 1977.
7. А. И. МАНЕВИЧ, *К теории связанной потери устойчивости подкрепленных тонкостенных конструкций*, Прикл. Математ. и Мех., 46, 2, 1982.
8. А. И. МАНЕБИЧ, *Устойчивость пластин и оболочек с ребрами таврового профиля*, Строительная Механика и Расчет Сооружений, 158, 2, 1985.
9. W. T. KOITER, A. van der NEUT, *Interaction between local and overall buckling of stiffened compression panels*, Part I, II, Thin-walled Structures J., Granada, London 1980.
10. Z. KOŁAKOWSKI, *Mode interaction in wide plate with closed sectional longitudinal stiffeners under compression*, Enging. Trans., **35**, 4, 1987.
11. Z. KOŁAKOWSKI, *Same aspects of mode interaction in thin-walled stiffened plate under uniform compression*, Enging. Trans., **36**, 1, 1988.
12. F. W. WILLIAMS, W. H. WITTRICK, *Numerical results for the initial buckling of some stiffened panels in compression*, Aeronaut. Quart., 23, 1972.
13. A. PFLÜGER, *Zum Beulproblem der anisotropen Rechteckplatte*, Ingenieur Archiv., 16, 1947.
14. S. P. CHANG, *Beitrag zur Berechnung des nichtlinearen Tragverhaltens einer in Längsrichtung mit offenen oder geschlossenen Steifen verstärkten und durch Druck belasteten Rechteckplatte mit Vorverformungen bei Navierschen Randbedingungen*, Dissertation, Universität Stuttgart, 1976.
15. Z. KOŁAKOWSKI, *Some thoughts of mode interaction in thin-walled column under uniform compression*, Thin-walled Structures, 7, 1989.

STRESZCZENIE

WSPÓŁDZIAŁANIE POSTACI WYBOCZENIA SZEROKIEJ PŁYTY WZMOCNIONEJ WZDŁUŻNYMI KĄTOWNIKAMI I PODDANEJ SCISKANIU

Rozważono problem współdziałania niemal równoczesnych postaci wyboczenia płyty wzmocnionej podłużnymi kątownikami o profilu cienkościennym. Zastosowano rozwinięcia asymptotyczne Byskova i Hutchinsona. Praca poświęcona jest pogłębionej analizie równowagi w początkowej fazie odkształceń ponadkrytycznych konstrukcji z imperfekcjami, z uwzględnieniem zjawiska współoddziaływania jednej globalnej oraz dwóch lokalnych postaci wyboczenia.

РЕЗЮМЕ

ВЗАИМОДЕЙСТВИЕ ВИДА ПРОДОЛЬНОГО ИЗГИБА ШИРОКОЙ ПЛИТЫ УПРОЧНЕННОЙ ПРОДОЛЬНЫМИ УГОЛЬНИКАМИ И ПОДВЕРГНУТОЙ СЖАТИЮ

Рассмотрена проблема взаимодействия почти одновременных видов продольного изгиба плиты, упрочненной продольными угольниками с тонкостенным профилем. Применены асимптотические разложения Быскова и Гаткинсона. Работа посвящена углубленному анализу равновесия в начальной фазе сверхкритических деформаций конструкции с имперфекциями, с учетом явления взаимодействия одного глобального и двух локальных видов продольного изгиба.

TECHNICAL UNIVERSITY OF ŁÓDŹ, ŁÓDŹ.

Received February 17, 1988.